Electronic Supplementary Information

Structural assignment of small cationic silver clusters by far-infrared spectroscopy and DFT calculations

Johan van der Tol,[a] Dewei Jia,[a] Yejun Li,[a,b] Valeriy Chernyy,[c] Joost Bakker,[c] Minh Tho Nguyen,[d] Peter Lievens,[a] Ewald Janssens[a]*

[a.] *Laboratory of Solid State Physics and Magnetism, KU Leuven, Celestijnenlaan 200 D, B-3001 Leuven, Belgium*

[b.] *Hunan Key Laboratory of Super Microstructure and Ultrafast Process, School of Physics and Electronics, Central South University, Changsha, Hunan 410083, P.R. China*

[c.] *Radboud University, Institute for Molecules and Materials, FELIX Laboratory, Toernooiveld 7c, 6525 ED Nijmegen, The Netherlands*

[d.] *Department of Chemistry, KU Leuven, Celestijnenlaan 200 F, B-3001 Leuven, Belgium*

[*] *E-mail: ewald.janssens@kuleuven.be*

Electronic supplementary information contains:

1. Assessment of the accuracy of computational levels using silver dimers and trimers (Table S1)

2. Ar adsorption sites and adsorption energies for Ag_3^+ and Ag_4^+, assessed using different functionals (Table S2 and Figure S1)

3. Effect of Ar adsorption on the vibrational spectrum of Ag_3^+ and Ag_4^+, assessed using different computational levels (Figures S2, S3, and S4)

4. Extended comparison of the infrared spectra of different isomers of Ag_n^+ (n = 10–15) with the experiment (Figures S5–S10)

5. Summary of bands for the identified structures in tables (Tables S3, S4, S5, and S6)

1. Assessment of the accuracy of computational levels using silver dimers and trimers

We assessed the accuracy of different functionals (TPSS and TPSSH) and different basis sets (LANL2DZ, Def2-TZVP, and AUG-CC-PVTZ-PP) on the smallest silver clusters Ag_2, Ag_3, Ag_2^+, and Ag_3^+ by comparison with spectroscopic results. In general, the pure TPSS functional gives better agreement with the experimental values than the hybrid TPSSH functional. Based on this comparison it was decided to use TPSS in conjunction with the Def2-TZVP basis sets. The triple zeta and split valence basis set Def2-TZVP includes 1p1d1f polarization for Ag and 2d1f for Ar, trimming off some diffuse functions from fully augmented sets. The corresponding effective core potentials (Def-ECP) are used.

Table S1. Vibrational frequencies and bond lengths of small Ag clusters, calculated at different levels, and comparison with experimental results.

	Ag_2^+		Ag_2		Ag_3^+	Ag_3
	bond length / Å	vibrational mode / cm^{-1}	bond length / Å	vibrational mode / cm^{-1}	vibrational mode / cm^{-1}	vibrational mode / cm^{-1}
TPSS/ LANL2DZ	2.755	130.1	2.573	190.51	116.0/118.2	120.9/180.7
TPSS/ Def2-TZVP	**2.738**	**129.0**	**2.559**	**191.02**	**120.0/121.5**	**119.7/183.6**
TPSS/ AUG-CC-PVTZ-PP	2.686	133.2	2.5727	190.9	124.7/126.7	135.05/184.8
TPSSH/ LANL2DZ	2.767	128.0	2.5773	189.1	115.6/117.4	117.5/177.6
TPSSH/ AUG-CC-PVTZ-PP	2.701	130.0	2.5776	189.0	123.2/125.0	118.0/186.8
Experiment	-	136.2±1 [1]	2.5310 [2]	192.4 [3]	130.0±1.2 [this work]	113/183 [4]

2. Ar adsorption sites and adsorption energies for Ag_3^+ and Ag_4^+, assessed using different functionals

The preferential binding site for Ar on Ag_3^+ and Ag_4^+ was assessed using different computational levels: i) the long range corrected hybrid functional LC-wPBE, ii) the long range corrected pure functional LC-TPSS, iii) the pure functional TPSS, and iv) the hybrid functional TPSSH, each in conjunction with the Def2-TZVP basis sets. LC-wPBE is a long range corrected hybrid functional developed by O. A. Vydrov *et al.* in 2006 based on PBE [5]. The long range corrected LC-TPSS was developed by Hirao and coworkers in 2001 [6].

Figure S1 shows three different adsorption sites for Ar on Ag_3^+. In structures (a) and (b) the Ar atom is located in the plane of the metal cluster, while it is out-of-plane in (c). Also for Ag_4^+ three adsorption sites are found. In structures (d) and (e) the Ar atom is in same plane as the atoms of the metal cluster, while it is out-of-plane in (f). The same preference for the Ar adsorption site on Ag_3^+ and Ag_4^+ is found at all different levels of calculation (see Table S2).
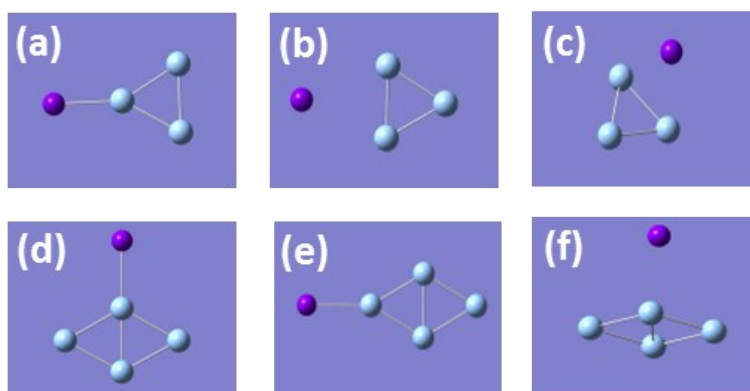
**Figure S1** Different Ar (purple sphere) attachment sites on Ag_3^+ (top) and Ag_4^+ (bottom)

Table S2 Ar binding energy and Ag-Ar bond length for different Ar adsorption sites on Ag_3^+ and Ag_4^+, assessed at different computational levels.

|		(a) Ag_3Ar^+	(b) Ag_3Ar^+	(c) Ag_3Ar^+	(d) Ag_4Ar^+	(e) Ag_4Ar^+	(f) Ag_4Ar^+
TPSS	Ar adsorption energy / eV	0.190	0.081	0.062	0.124	0.088	0.030
	Ag–Ar bond length / Å	2.763	3.626	4.463	2.814	2.921	4.621
TPSSH	Ar adsorption energy / eV	0.145	0.049	0.032	0.111	0.077	0.026
	Ag–Ar bond length / Å	2.770	3.659	4.546	2.831	2.941	4.602
LC-TPSS	Ar adsorption energy / eV	0.173	0.031	0.007	0.128	0.090	0.016
	Ag–Ar bond length / Å	2.63	3.523	4.239	2.763	2.726	4.04
LC-wPBE	Ar adsorption energy / eV	0.187			0.163		
	Ag–Ar bond length / Å	2.767			2.806		

3. Effect of Ar adsorption on the vibrational spectrum of Ag_3^+ and Ag_4^+, assessed using different computational levels

Figures S2 and S3: Calculated infrared absorption spectra of the most preferred Ag_3^+Ar (structure (a) in figure S1) and Ag_4^+Ar (structure (d) in figure S1) calculated at different computational levels: TPSSH/Def2-TZVP, TPSS/Def2-TZVP, LC-wPBE/Def2-TZVP, and LC-TPSS/Def2-TZVP. This comparison demonstrates the effect of the functional on the vibrational modes in the spectral range of the experiment.

Figure S4: Infrared absorption spectra of the cluster–argon complexes of $Ag_4Ar_m^+$ (m = 1–4), calculated at the TPSSH/Aug-CC-PVTZ-PP level, illustrating the effects of the number adsorbed argon atoms and on the preferred adsorption sites. One can note the significant differences in the intensities of the vibrational modes for the different spectra, while the frequencies are nearly unaffected when adding more Ar atoms or when varying the adsorption sites.
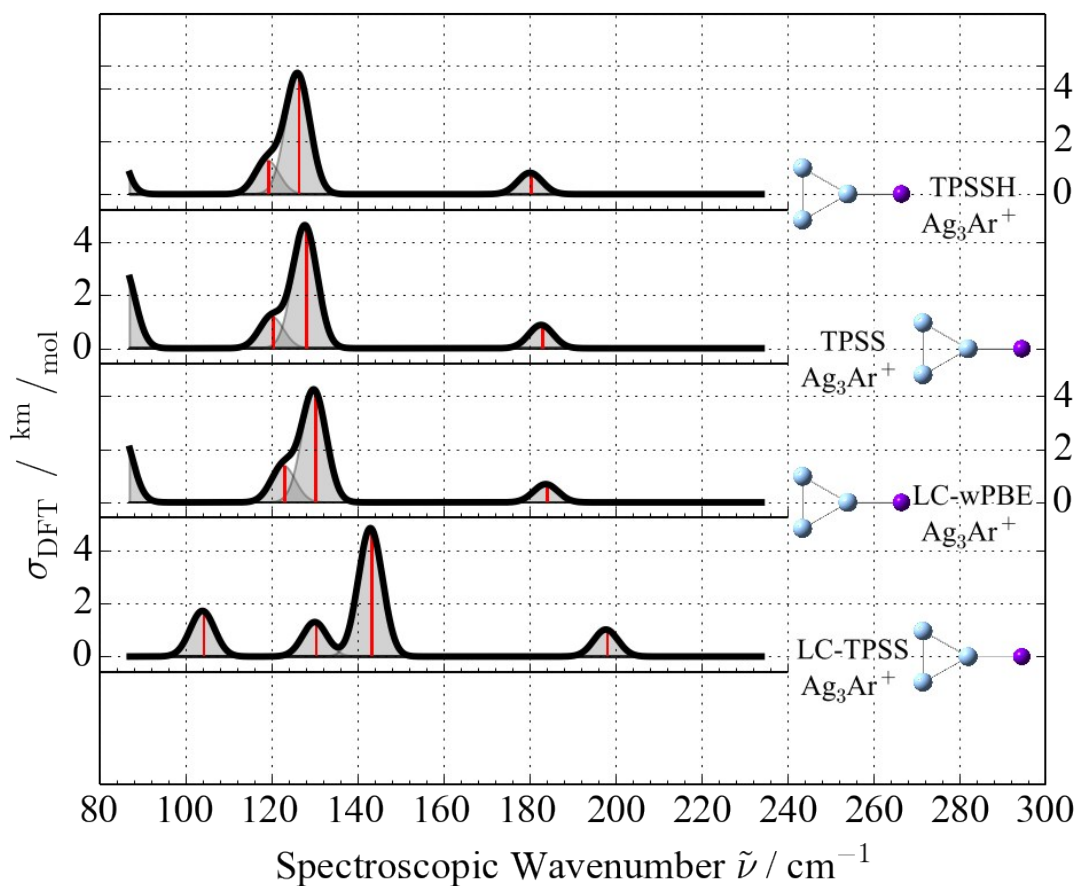
Figure S2 Harmonic infrared spectra of the most stable structure of the Ag_3Ar^+ complex (structure (a) in Figure S1), calculated using the TPSS, TPSSH, LC-TPSSH, LC-wPBE functionals.

4
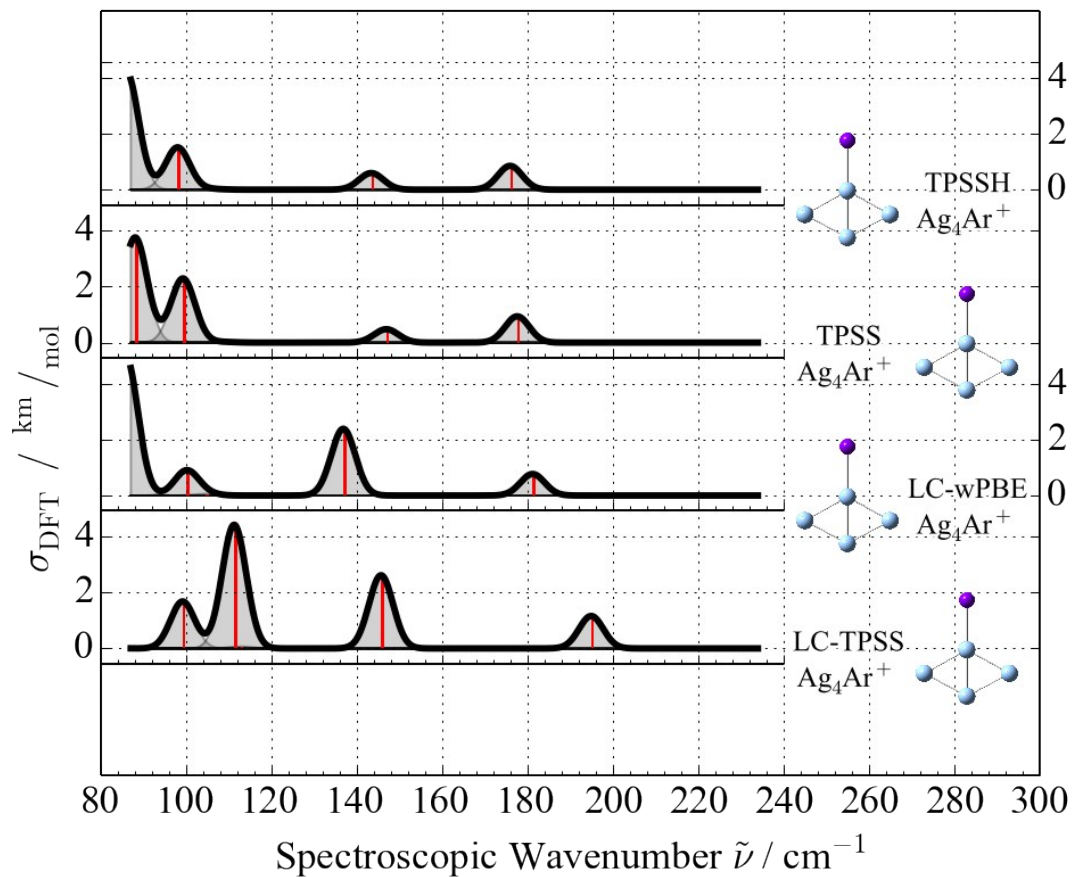
Figure S3 Harmonic infrared spectra of the most stable structure of the Ag$_4$Ar$^+$ complex (structure (d) in Figure S1), calculated using the TPSS, TPSSH, LC-TPSSH, LC-wPBE functionals.
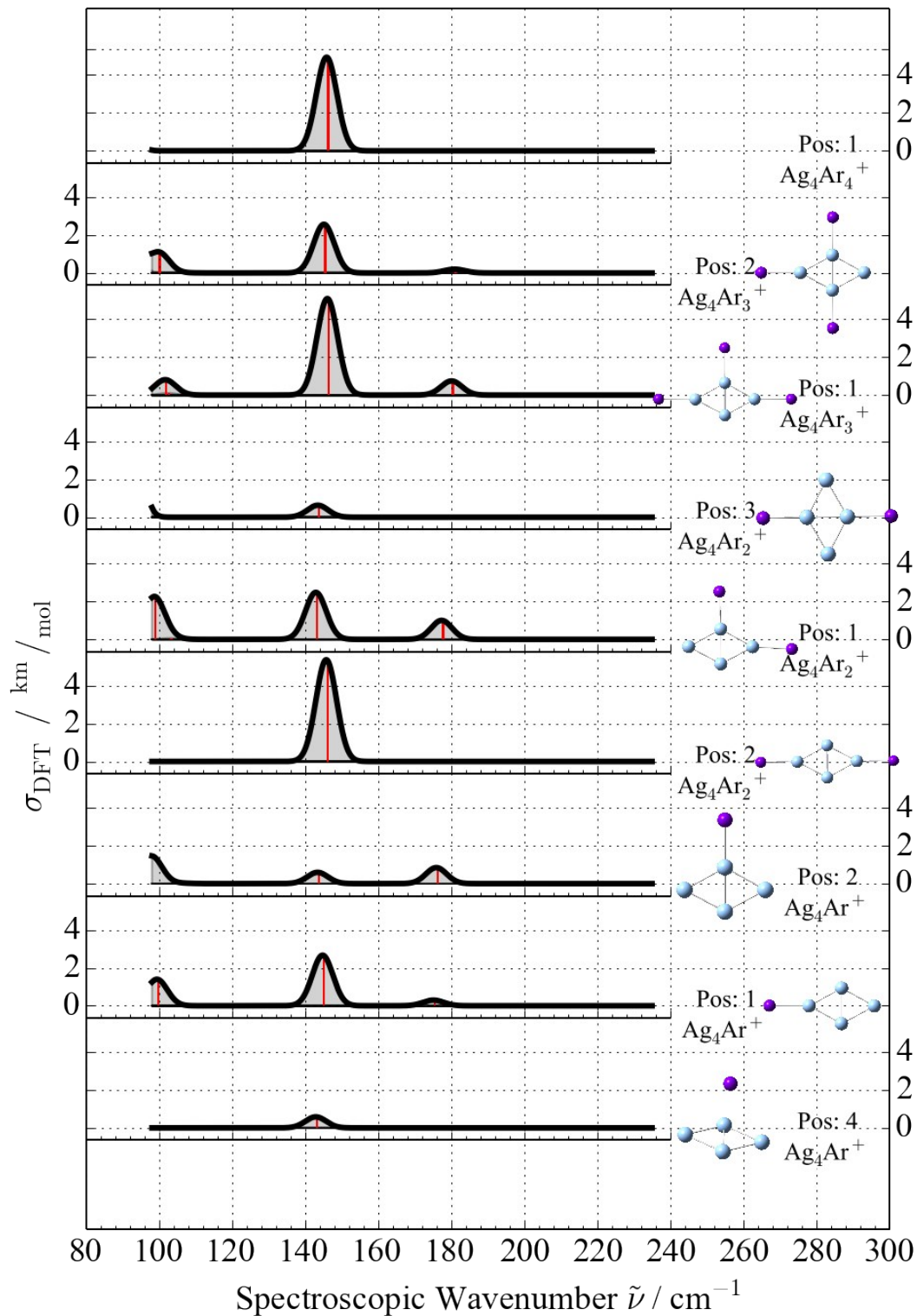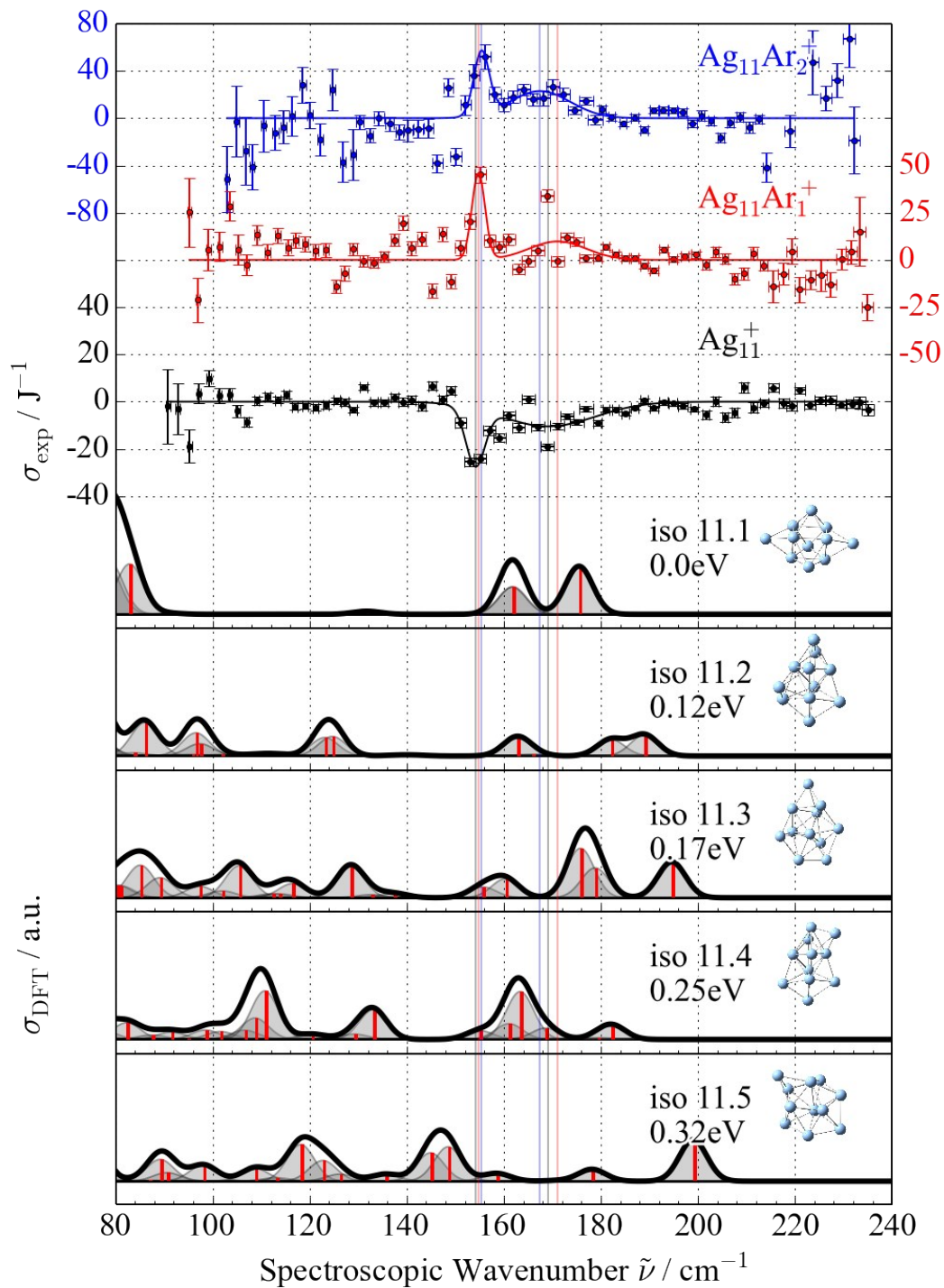
Figure S4 Calculated harmonic infrared spectra of the $Ag_4Ar_2^+$ complex for different adsorption sites of the Ar atoms, as calculated at the TPSSH/Aug-CC-PVTZ-PP level.

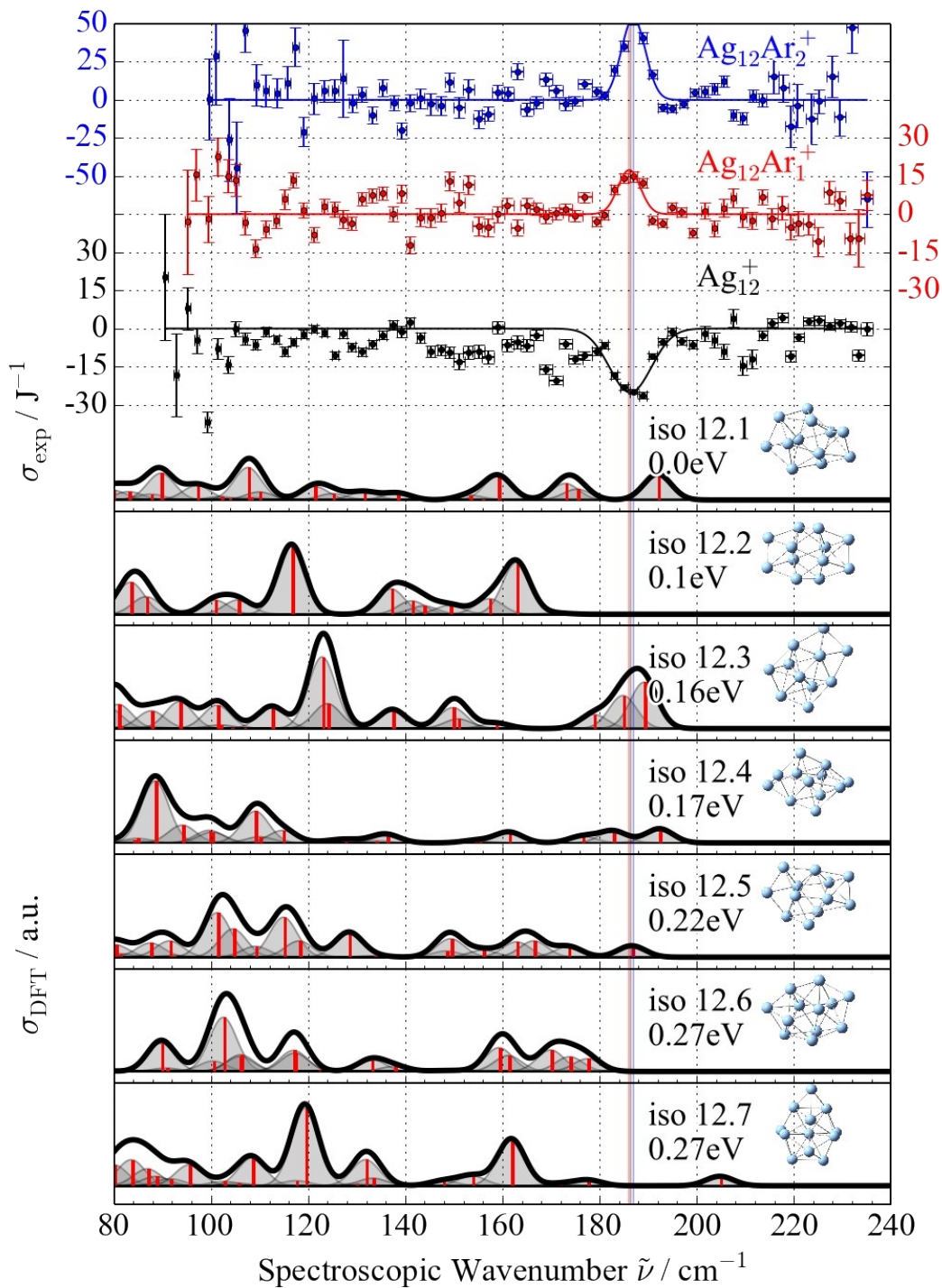## 4. Extended comparison of the infrared spectra of different isomers of Ag_n^+ (n = 10–15) with the experiment
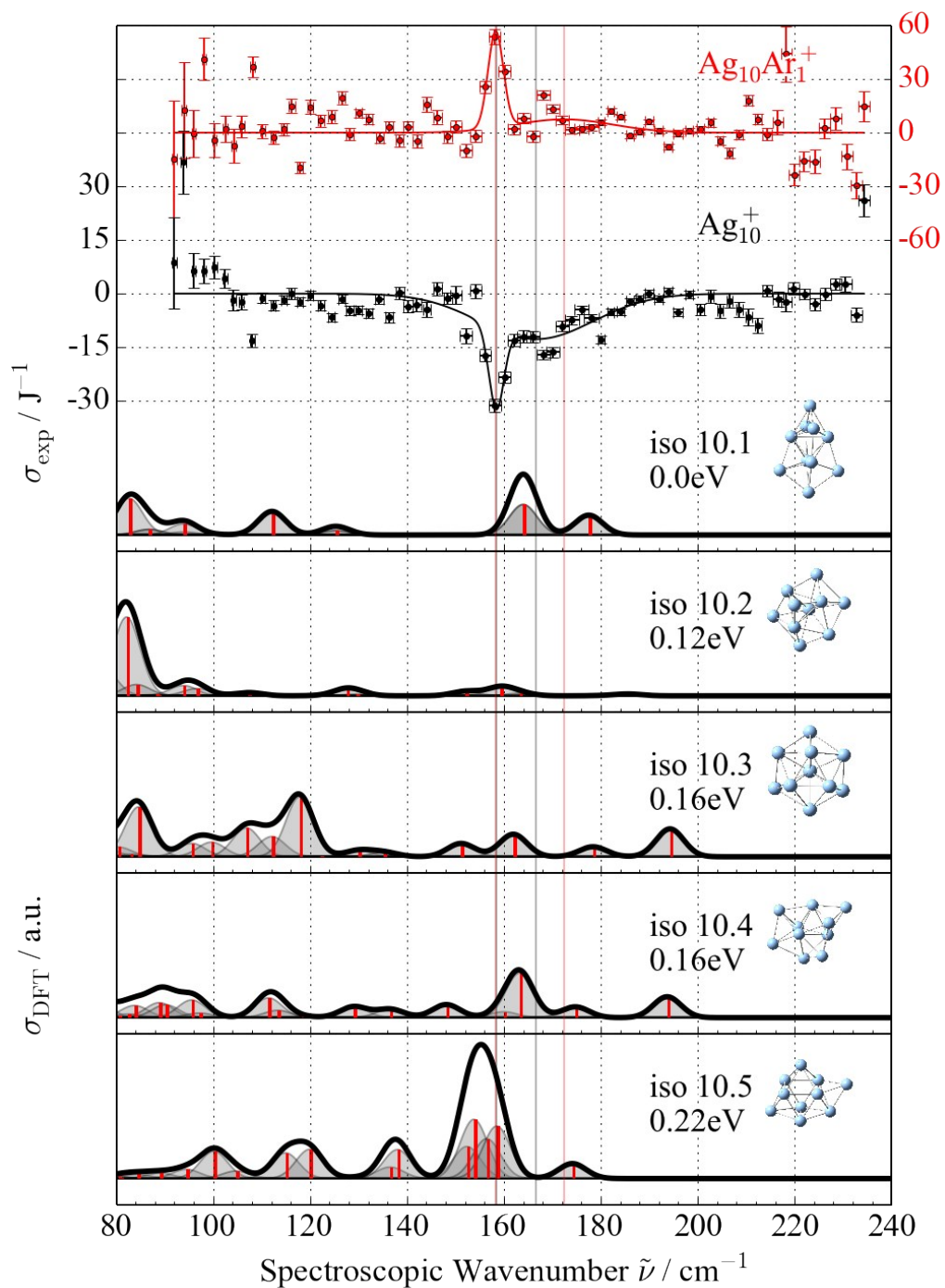
Figure S5. Comparison of the experimental cross sections of $Ag_{10}Ar^+$ complexes with calculated harmonic infrared spectra for several structural isomers of Ag_{10}^+.
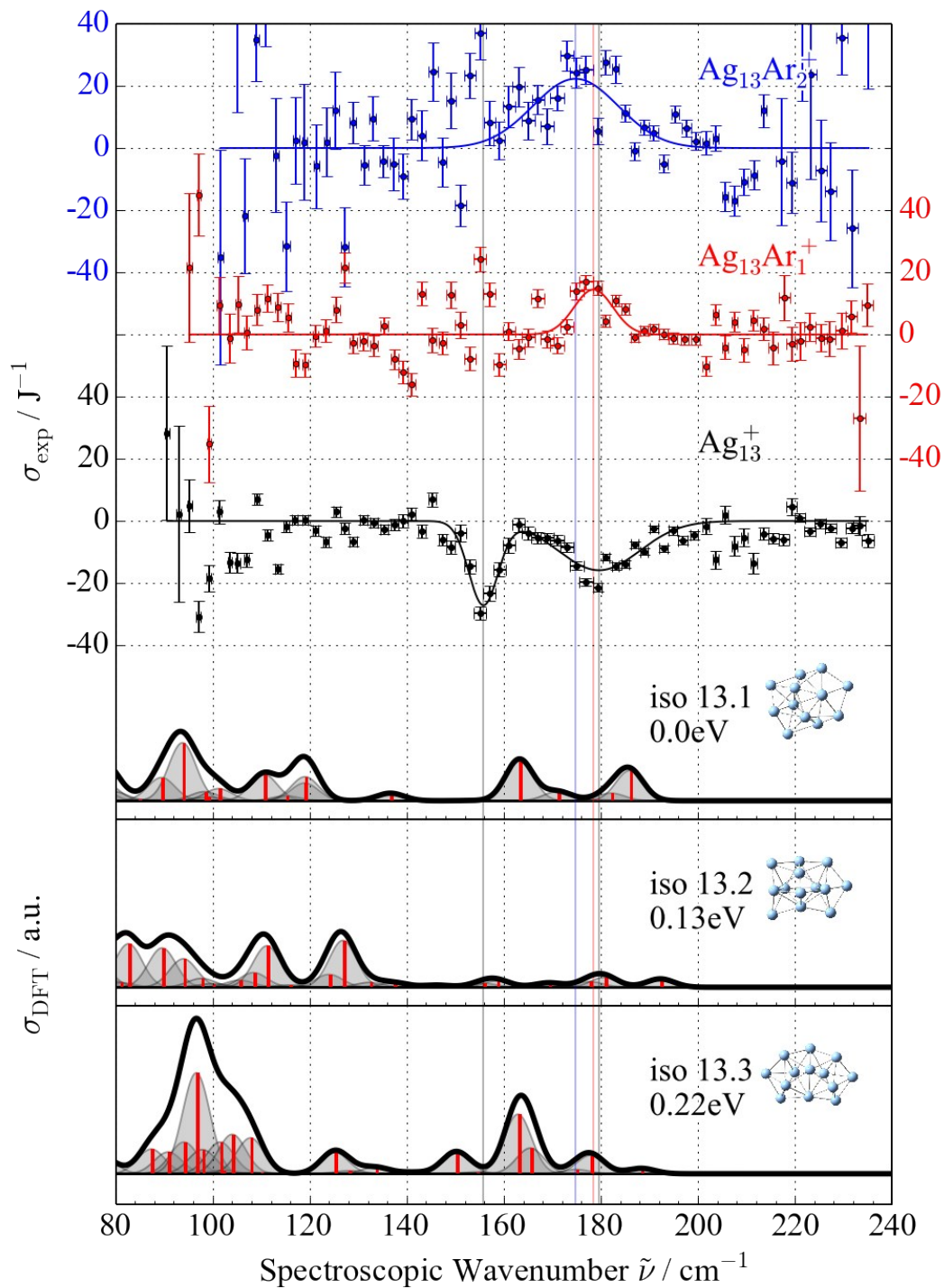
Figure S6. Comparison of the experimental cross sections of $Ag_{11}Ar^+$ and $Ag_{11}Ar_2^+$ complexes with calculated harmonic infrared spectra for several structural isomers of Ag_{11}^+.
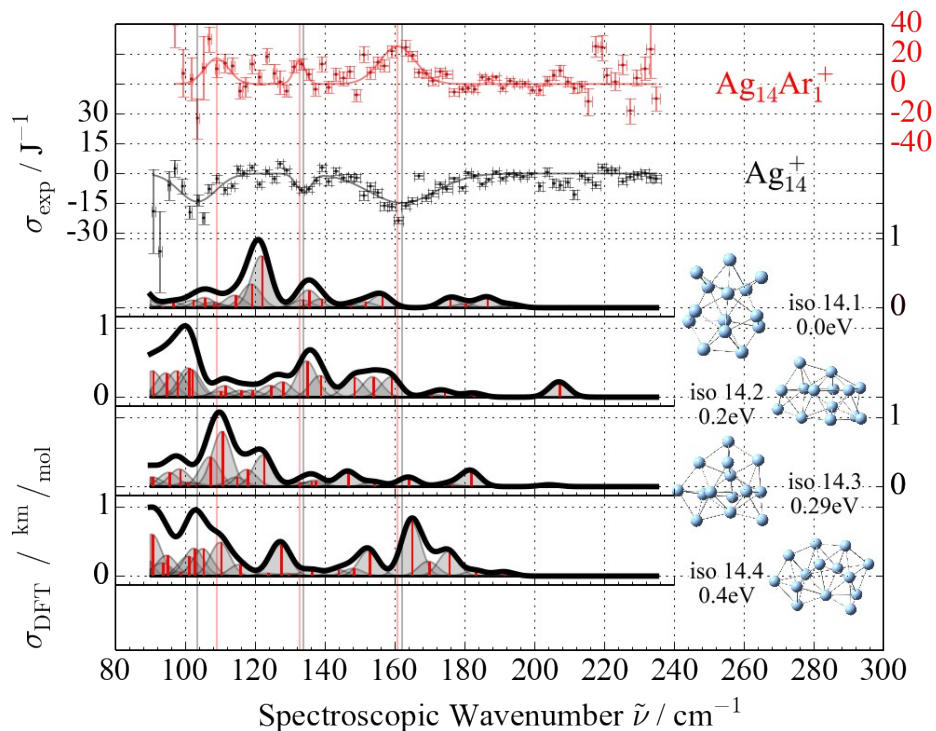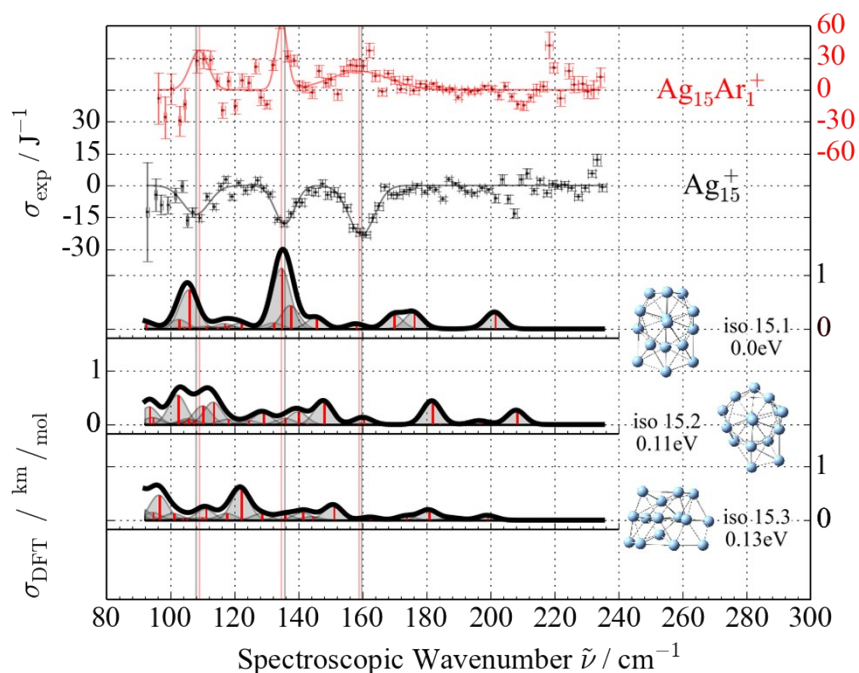
Figure S7. Comparison of the experimental cross sections of $Ag_{12}Ar^+$ and $Ag_{12}Ar_2^+$ complexes with calculated harmonic infrared spectra for several structural isomers of Ag_{12}^+.

Figure S8. Comparison of the experimental cross sections of $Ag_{13}Ar^+$ and $Ag_{13}Ar_2^+$ complexes with calculated harmonic infrared spectra for several structural isomers of Ag_{13}^+.

Figure S9. Comparison of the experimental cross sections of Ag$_{14}$Ar$^+$ complexes with calculated harmonic infrared spectra for several structural isomers of Ag$_{14}^+$.

Figure S10. Comparison of the experimental cross sections of Ag$_{15}$Ar$^+$ complexes with calculated harmonic infrared spectra for several structural isomers of Ag$_{15}^+$.

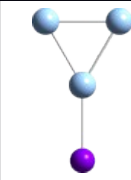We remark that we saw a clear band at (160 ± 5) cm^{-1} for Ag$_n^+$ (n=19, 20, 21), as well as a band at (115 ± 5) for Ag$_{19}^+$

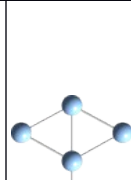## 5. Summary of bands for the identified structures in tables

For a more precise identification of the measured bands, tables with fitted numbers are provided. The reported uncertainties correspond to the fit-uncertainties of the fitted gaussians.

Table S3 $Ag_3Ar_m^+$ and $Ag_4Ar_m^+$

$Ag_3Ar_m^+$
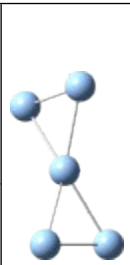
m	Exp/cm^{-1}	DFT/cm^{-1}	
4	130.0 ± 1.2		
	↓	120.0	
2	129.3 ± 0.8	127.9	
1	126.1 ± 1.0		

$Ag_4Ar_m^+$
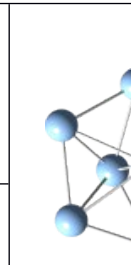
m	Exp/cm^{-1}	DFT/cm^{-1}	
4	143.2 ± 0.9		
3	141.3 ± 0.8		
	↓	146.9	
2	143.2 ± 0.8		
1	142.8 ± 1.6		
3	<100		
	↓	87.9	
2	91 ± 6	99.1	
1	92 ± 4		

Table S4 $Ag_5Ar_m^+$ and $Ag_6Ar_m^+$

$Ag_5Ar_n^+$

m	Exp/cm^{-1}	DFT/cm^{-1}	
3	117.4 ± 1.7		
2	113.6 ± 1.7		
1	114.9 ± 1.4	105.0	
	↓		
0	114.2 ± 1.0		
3	146.7 ± 1.7		
2	146.4 ± 1.1	143.8	
	↓		
0	146.4 ± 0.7		

$Ag_6Ar_n^+$
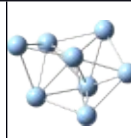
m	Exp/cm^{-1}	DFT/cm^{-1}	
3	103 ± 16	104.4	
	↓		
2	106 ± 7		
3	126.4 ± 1.2	132.8	
	↓		
2	126.1 ± 1.2		

Table S5 $Ag_7Ar_n^+$ and $Ag_8Ar_n^+$

$Ag_7Ar_m^+$
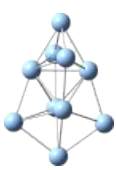
m	Exp/cm^{-1}	DFT/cm^{-1}	
2	102 ± 3	97.7	
	↓		
1	103.6 ± 1.1		

$Ag_8Ar_m^+$
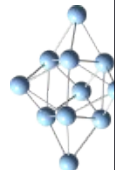
m	Exp/cm^{-1}	DFT/cm^{-1}	
2	182.2 ± 0.8		
1	182.6 ± 0.7	185.4	
	↓		
0	182.1 ± 1.0		

Table S6 $Ag_{10}Ar_m^+$ and $Ag_{11}Ar_m^+$

$Ag_{10}Ar_m^+$

m	Exp/cm^{-1}	DFT/cm^{-1}	
1	158.4 ± 0.7	163.9	
	↓	164.0	
0	158.4 ± 0.8		
2	165 ± 4		
1	169.0 ± 1.5	177.5	
	↓		
0	167 ± 4		

$Ag_{11}Ar_m^+$
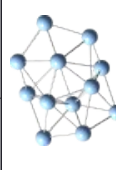
m	Exp/cm^{-1}	DFT/cm^{-1}	
2	155.4 ± 1.2	161.7	
1	154.8 ± 0.7	161.9	
	↓		
0	154.1 ± 0.8		
2	167 ± 4		
	↓	175.5	
0	169 ± 4		

Table S7 $Ag_{12}Ar_m^+$ and $Ag_{13}Ar_m^+$

$Ag_{12}Ar_m^+$

m	Exp/cm^{-1}	DFT/cm^{-1}
2	187.0 ± 0.5 186.1	Multiple isomers competing
1	± 0.9	
	↓	
0	186.4 ± 1.1	

$Ag_{13}Ar_m^+$
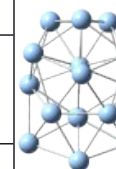
m	Exp/cm^{-1}	DFT/cm^{-1}	
2	175 ± 3		
1	178.5 ± 1.7	185.9	
	↓		
0	180 ± 2		
	?		
	↓	163.2	
0	155.8 ± 1.3		

Table S8 $Ag_{14}Ar_m^+$ and $Ag_{15}Ar_m^+$

$Ag_{14}Ar_n^+$

m	Exp/cm^{-1}	DFT/cm^{-1}
1	109 ± 6	
	↓	
0	104 ± 4	Multiple isomers competing
1	160.8 ± 1.8	
	↓	
0	162 ± 3	

$Ag_{15}Ar_n^+$

m	Exp/cm^{-1}	DFT/cm^{-1}	
1	109 ± 4	105.6	
	↓		
0	108 ± 4		
1	134.8 ± 0.8	134.6	
	↓	137.4	
0	135.6 ± 1.6		
1	159 ± 5		
	↓	-	
0	159.7 ± 1.3		

References

[1]   G. I. Nemeth, H. Ungar, C. Yeretzian, H. L. Selzle, E. W. Schlag, High-resolution spectroscopy of Ag_2^+ via long-lived ZEKE states, *Chem. Phys. Lett*., 1994, **228**, 1-8.

[2]   B. Simard, P. A. Hackett, A. M. James, P. R. R. Langridge-Smith The bond length of silver dimer, *Chem. Phys. Lett*. 1991, **186**, 415-422.

[3]   V. Beutel, M. Kuhn, W. Demtröder, *Rotationally resolved isotope-selective laser spectroscopy of the Ag_2 molecule, J. Mol. Spectrosc.*, 1992, **155**, 343-351.

[4]   A. Fielicke, I. Rabin, G. Meijer, Far-infrared spectroscopy of small neutral silver clusters, *J. Phys. Chem. A*, 2006, **110**, 8060–8063.

[5]   O. A. Vydrov, G. E. Scuseria, Assessment of a long-range corrected hybrid functional, *J. Chem. Phys.* 2006, 125, 234109.

[6]   H. Iikura, T. Tsuneda, T. Yanai, K. Hirao, A long-range correction scheme for generalized-gradient-approximation exchange functionals, *J. Chem. Phys.*, 2001, **115**, 3540-3544.